ARTICLES

Pressure Shift Mechanisms of Spectral Holes in the Optical Spectra of Dyes in Polymer Host Matrices[1]

Indrek Renge*

Institute of Physics, Tartu University, Riia 142, EE51014 Tartu, Estonia

Received: September 2, 1999; In Final Form: January 26, 2000

The influence of hydrostatic pressure (P) up to 200 bar of gaseous He was investigated on holes burned over the inhomogeneous $S_1 \leftarrow S_0$ absorption bands of polycyclic hydrocarbons, a polymethine dye, and tetrapyrrolic compounds imbedded in polymer matrices. The pressure shift coefficients $d\nu/dP$ show a linear dependence on hole burning frequency (ν) that can be extrapolated to the frequency $\nu_{0(P)}$ where no pressure shift occurs. The $\nu_{0(P)}$ values deviate significantly from the actual 0−0 origins of the nonsolvated chromophores. The dependence of $d\nu/dP$ on ν can be considerably steeper than the 2-fold isothermal compressibility of the matrix $2\beta_T$, expected for the distance dependence of intermolecular potential r^{-6} (e.g. London forces). Other solvent shift mechanisms, such as linear and quadratic Stark effects in the matrix cavity field, yield lower slope values than $2\beta_T$ ($^1/_3\beta_T$ and $^2/_3\beta_T$, respectively). Tentatively, these controversies are rationalized in terms of intermolecular repulsive interactions that have a much steeper distance dependence (r^{-12}) than the electrostatic or dispersive forces. The solvent shifts of band maxima, the inhomogeneous bandwidths, and the pressure shifts of spectral holes are discussed in terms of intermolecular interaction mechanisms.

Introduction

Considerable attention has been paid to the optical spectra of chromophores in polymer matrices under very high pressures (P) up to 40−150 kbar, including the main groups of organic dyes and pigments: polyenes,[2] polymethine dyes,[3] polyarenes,[4,5] and tetrapyrroles,[6] as well as several heteroaromatic compounds.[7] In most papers, the spectra have been measured at room temperature using large steps of the P change of 5−20 kbar. At high P structural changes occur in the noncrystalline systems, such as the collaps of free volume. The irreversible phenomena remained almost unnoticed in earlier papers. Recently the memory effects in amorphous materials after the first compression cycle up to several kilobar have been documented at low temperatures by means of spectral hole burning.[8] Since the holes are at least by a factor of 10^3 narrower than the inhomogeneous bands, the influence of small pressure changes can be easily studied. Hole burning offers the possibility to explore the chromophores selected by energy, whereas the system remains in an elastic deformation regime. The first studies of both hydrostatic and uniaxial pressure were carried out on phthalocyanine doped in polymer host matrices.[9,10] From the P shifts of holes burned close to the band maxima the isothermal compressibilities (β_T) were obtained that are close to the values of the bulk material.[11] However, instead of the sequence of β_T values decreasing as polystyrene (PS) > polyethylene (PE) > poly(methyl methacrylate) (PMMA),[11] the following one was obtained from the optical measurement: PMMA > PS > PE.[10]

A model was developed soon with the aim of getting a microscopic insight into the P effects in the hole burning experiment.[12] It was predicted that the P shift will depend on the position within the inhomogeneous spectral contour. Such color effect was observed soon on resorufin in alcohol glass.[13] It was shown that the slope of the dependence of the P shift coefficient $d\nu/dP$ vs the burning wavenumber (ν) should be equal to $2\beta_T$ and that the frequency where no P shift occurs gives the 0−0 origin of the nonsolvated chromophore (ν_0).[13,14] Experimentally, it was established for different dopants (protoporphyrin, resorufin, hypericin, dimethyl-*s*-tetrazine) that in ethanol−methanol glass the slopes are rather similar to each other ($(3.1 \pm 0.2) \times 10^{-5}$ bar^{-1}).[14] Unfortunately, the β_T values for solvent glasses are not available, so no check was possible. For most of the dyes the vacuum frequencies in supersonic jets have not been measured, so the direct comparison between ν_0 and the extrapolated zero-pressure-shift frequency ($\nu_{0(P)}$) could not be done. Despite these problems, further work has been dedicated to the determination of protein compressibilities with the aid of this procedure.[15,16]

Since the low-temperature compressibilities of a number of polymers are known,[11] it appeared to us challenging to test the hole burning method in a more extensive fashion by using tetra-*tert*-butylporphyrazine (*t*-Bu-TAP) as a probe. Between $2\beta_T$ and the slopes of P shift coefficients vs hole frequency a satisfactory agreement was found, but the extrapolated vacuum frequencies showed a very large scatter. On the other hand, several other π-electronic chromophores were measured in a single matrix, PMMA. Here another major controversy was revealed for nonpolar polycyclic hydrocarbons that are expected to possess the simplest solvent shift behavior. In addition to the poor correspondence between ν_0 and $\nu_{0(P)}$, slopes considerably larger than $2\beta_T$ were obtained.

* Phone: +3727-428882; +3727-304800. FAX: +3727-383033. E-mail: renge@fi.tartu.ee.

10.1021/jp9931206 CCC: $19.00
Published on Web 04/08/2000

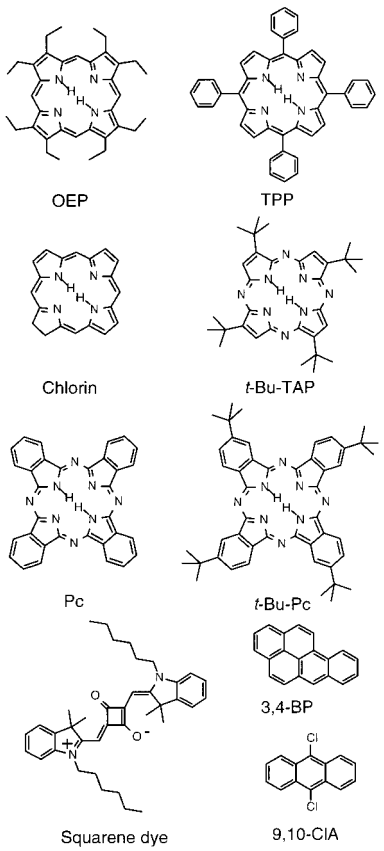

Figure 1. Chemical structures of guest molecules.

The failure of idealized model considerations stimulated us to investigate the interrelationships between the solvent shifts[17−19] and the *P* effects on spectral holes in more detail. Liquid-phase studies in the solvent sets with gradually varying polarities and polarizabilities enable one to specify the solvent shift mechanisms and yield the vacuum frequencies for those dyes that are difficult to measure in supersonic jets.[17−19] The microscopic solvent shift mechanisms also determine the inhomogeneous band broadening.[20] The following interactions will be analyzed in this work: the exchange repulsion, the attractive London forces, the linear and quadratic Stark effects in the cavity and reaction fields, and finally, the peculiar solvation of the center of free-base tetrapyrrolic pigments.[18,19] The term "peculiar" has been applied, since the "specific solvation" refers to the hydrogen bonding and the charge-transfer complexation phenomena.[21] The influence of solvatochromic mechanisms on the inhomogeneous widths and the *P* shift coefficients will be discussed.

Experimental Section

The properties of polymers (mostly from Aldrich) and the sample preparation were described in our previous paper.[22] The squarene dye was provided by T. L. Tarnowski (Syntex, Palo Alto, CA), chlorin by G. Grassi (ETHZ), and the remaining compounds by Aldrich. The chemical structures of the guest molecules are depicted in Figure 1. The samples consisted of 0.1−1 mm thick polymer films doped with the dyes to the optical density of 0.5−2 at the $S_1 \leftarrow S_0$ maximum. Absorption spectra were recorded on a Perkin-Elmer Lambda 9 spectrophotometer. Pressure shift studies were carried out in a simple cell that can be filled with gaseous He up to 200 bar. The cell body consists of a stainless steel cylinder of 20 mm diameter, housing a sample volume of $2 \times 4 \times 4$ mm^3. The samples were loaded to a precooled CF1204 continuous flow cryostat (Oxford). To avoid the temperature rise upon the application of He gas pressure, the hole burning was performed at a maximum *P* of about 200 bar at 5−8 K. Then the gas bottle valve was closed, and the influence of pressure change was followed by releasing He gas in five to eight steps.

Holes were burned with Lambda Physik dye laser LPD 3002E (line width, 2.5 GHz; pulse length, ∼10 ns) pumped with an excimer laser LPX 100. Relatively deep holes broadened by the light dose were created at three to five frequencies over the band during a single pressure run. Holes were explored in transmission by applying the same laser with an attenuated pulse energy. A two-channel Molectron JD2000 Joulemeter Ratiometer was used with a sensitive (10^9 V/J) J3S-10 probe in the sample channel and a less sensitive one (10^3 V/J), J3-09, as a reference. The signals of the two channels were divided, averaged over 10 pulses, and fed into the SUN computer. Typically 400 data points per scanning interval were collected. Only the pressure induced shifts will be described in the present paper; the broadening will be treated in a separate publication.

Model Considerations

(1) Dependence of Pressure Shift Coefficients on Hole Burning Frequency in Nonpolar Systems. The dispersion interaction is responsible for bathochromic shifts in many less polar molecular guest−host systems. Absorption band maxima of not very polar chromophores in apolar medium obey well the Bakhshiev equation:[17,23−25]

$$\nu_{max} = \nu_0 + p\phi(n^2)$$

$$p = -3II'(\alpha_e - \alpha_g)/[2(I + I')a^3]$$

$$\phi(n^2) = (n^2 - 1)/(n^2 + 2) \qquad (1)$$

where ν_{max} and ν_0 are the peak wavenumbers in the condensed and gas phases, respectively, I and I' are the ionization energies of the solute and solvent molecules, $\alpha_e - \alpha_g = \Delta\alpha$ is the average static polarizability difference between the excited (e) and the ground (g) states, a is the Onsager cavity radius, and n is the refractive index of the solvent for the Na D line. The Lorentz−Lorenz function $\phi(n^2)$ is linearly related to the density of the solvent d:[26]

$$\phi(n^2) = (4\pi N_A \alpha_s/3M_w)d \qquad (2)$$

where N_A is the Avogadro number, α_s is the polarizability of the solvent molecule, and M_w is the molecular weight. Thus, $\phi(n^2)$ can be expressed through the mean volume per molecule or, in case of polymers, per repeating unit, V_m:

$$\phi(n^2) = 4\pi\alpha_s/3V_m \qquad (3)$$

Both V_m and the Onsager volume V_O ($V_O = 4\pi a^3/3$) may be regarded as unit volume V multiplied by constants. Denoting all constants in eq 1 as c_1, one obtains for the absolute solvent shift

$$\nu_{max} - \nu_0 = c_1 V^{-2} \qquad (4)$$

Because compression of the matrix under hydrostatic pressure influences both $\phi(n^2)$ and a^3, the solvent shift scales with respect to the volume as V^{-2}. The pressure shift of the band maximum at fixed temperature equals

$$d\nu_{max}/dP = -2c_1(dV/dP)_T V^{-3} \quad (5)$$

Since $c_1 = (\nu_{max} - \nu_0)V^2$ (eq 4) and the isothermal compressibility of the medium β_T is $-(dV/dP)_T V^{-1}$, one gets

$$d\nu_{max}/dP = 2\beta_T(\nu_{max} - \nu_0) \quad (6)$$

Strictly speaking, it follows from the above derivation that eq 6 applies to the pressure shift of a band maximum or a spectral hole burned at the peak positions. Similarly, it should be correct for groups of molecules selected by energy using hole burning within the inhomogeneous spectral band:

$$d\nu/dP = 2\beta_T(\nu - \nu_0) \quad (7)$$

Alternatively, eq 7 can be deduced from microscopic models[12,13] if the intermolecular potential changes as r^{-6} (as in the case of dispersion forces).

(2) Dependence of Pressure Shift Coefficients on Hole Burning Frequency in Polar Hosts. The electric field E of a cavity formed in a polar host matrix produces both linear and quadratic Stark effects on the impurity spectra:

$$\Delta\nu = \Delta\mu E \cos\varphi + {}^1/_2\Delta\alpha E^2 \quad (8)$$

where $\Delta\nu$ is the frequency shift, $\Delta\mu$ is the dipole moment difference between the ground and the excited states, and φ is the angle between $\Delta\mu$ and E.

Because the direction of the cavity field with respect to the permanent dipole moment difference vector of the solute is oriented randomly, no shift of the band maximum is expected for the linear effect. Instead, a strong band broadening takes place because on the average half of the molecules undergo a bathochromic shift and the other half a hypsochromic one.[20]

In centrosymmetric chromophores ($\Delta\mu = 0$) the linear Stark effect vanishes. We have proposed an empirical relationship for the quadratic Stark shift[27] of band maxima in polar solvents in terms of the polarizability difference $\Delta\alpha$ and the solvent dielectric permittivity function $\phi(\epsilon) - \phi(n^2)$, where $\phi(\epsilon) = (\epsilon - 1)/(\epsilon + 2)$.[28]

In addition to the purely stochastic matrix cavity field, the molecules with ground-state dipole moment (μ_g) create a reaction field that is proportional and collinear with μ_g.[23,26] The interaction of this field with the vector difference $\Delta\mu$ produces a net transition frequency shift that can be either to the blue or to the red, depending on the magnitude and mutual orientation of the ground- and the excited-state dipole moments.[23] However, the linear Stark effect in the reaction field is of little significance in hole burning systems, since appreciable change in molecular dipole moments results in such a dramatic decrease of the Debye−Waller factor that the observation of zero-phonon holes becomes difficult.[29]

Under pressure both the cavity and reaction field strengths scale with the sample volume (V) as ${}^1/_3V$. Therefore, a rather shallow dependence of pressure shift coefficients as a function of hole position is expected for the systems where only the inhomogeneous electric fields produce band broadening: ${}^1/_3\beta_T$ for the linear Stark effect and ${}^2/_3\beta_T$ for the quadratic Stark effect (Table 1).

(3) Dependence of Pressure Shift Coefficients on Repulsive Potentials. The reality of both attractive and repulsive forces between the molecules follows from the very existence of molecular condensed matter. However, the role of electrostatic or exchange repulsion on impurity spectra has remained elusive. In the case of atomic solids, e.g. individual Na or Hg atoms dispersed in rare gas matrices, the spectral blue shifts have been accounted for in terms of repulsive interactions that are stronger in the excited state than in the ground state.[30] Such a blue shift appears to be rarely documented for molecular systems.[17,31] Among the few exceptions is the pressure induced blue shift of the ^1L_b transition of benzene in liquid perfluorohexane.[32] As a rule, progressive bathochromic shifts take place even at very high pressures, revealing no hint to the above-mentioned blue shift of repulsive origin.[2−7]

The difficulties of separating the attractive and repulsive interactions become obvious from Figure 2, showing the intermolecular potential energy for a pair of spherical molecules as a function of distance. A continuous intermolecular potential is separable into components as far as the model curves for each are defined. The magnitude of either repulsive or attractive energy depends on the model potentials chosen. In the excited states of many nonpolar systems the upper minimum is deeper and the attractive branch is steeper due to the higher polarizability of the excited state that in its turn enhances the London forces. The situation with the repulsive part is less clear. Regarding the increase of molecular polarizability in terms of the volume increase of the electron cloud, one reaches the above-mentioned conclusion about the repulsive blue shift. However, the opposite effect is also conceivable, bearing in mind the possibility of partial electron transfer to the solvent and its delocalization in the excited state (the exciplex phenomenon). Thus, the repulsive branch in the upper state can be shallower as well.

The intermolecular repulsive potential has a steep distance dependence as r^{-12}, according to Lennard-Jones approximation. At present, it is just a speculation to assume that the solvent shift regarded as a difference between the repulsion energies in the ground and in the excited states obeys a similar dependence. However, if we accept this, the frequency shift may be expressed as

$$\nu - \nu_0 = c_2 r^{-12} \quad \text{or} \quad \nu - \nu_0 = c_3 V^{-4} \quad (9)$$

where c_2 and c_3 are the constants and V is the unit volume. The pressure shift can be found as already described above:

$$d\nu/dP = -4c_3(dV/dP)_T V^{-5} \quad \text{or} \quad d\nu/dP = 4\beta_T(\nu - \nu_0) \quad (10)$$

In summary, the total shift of a spectral hole vs the 0−0 origin of a free chromophore may be split into components:

$$\Delta\nu = \Delta\nu_{disp} + \Delta\nu_{Stark1} + \Delta\nu_{Stark2} + \Delta\nu_{rep} \quad (11)$$

The corresponding P shift may be expressed as follows:

$$d\nu/dP = (2\Delta\nu_{disp} + {}^1/_3\Delta\nu_{Stark1} + {}^2/_3\Delta\nu_{Stark2} + 4\Delta\nu_{rep})\beta_T \quad (12)$$

Therefore, the magnitudes of solvent shift components should be known at least qualitatively in order to understand the pressure effects on spectral holes in general, and the shift coefficient $d(d\nu/dP)/d\nu$ in particular.

Results and Discussion

(1) Solvent Shift Mechanisms. The simplest way to elucidate the universal, nonspecific solvation mechanisms is to study the optical spectra in liquid solvents of various dielectric properties.[21,23] In particular, the dependence of band maxima on $\phi(n^2)$ (eq 1) is perfectly linear when measured in a set of liquid

TABLE 1: Solvent Shift, Inhomogeneous Broadening, and Pressure Shift Mechanisms of Optical Transition Energies[a]

interaction type	microscopic shift	shift of band maximum ($\nu_{max} - \nu_0$)[b] (cm^{-1})	inhomogeneous width (FWHM)[b]	d(dP/dν)/dν[c]
dispersive attraction	$\sim(\alpha_s\Delta\alpha)/r^6$	$-(6.0 \times 10^4\Delta\alpha/M_w)[\phi(n^2)]$	$\sim 0.1(\nu_{max} - \nu_0)$	$2\beta_T$
linear Stark effect in the cavity field	$\sim(\mu_g - \mu_e \cos\gamma)E \cos\varphi$	0	$\sim(\mu_g - \mu_e \cos\gamma)[\phi(\epsilon) - \phi(n^2)]^{1/2}$[d]	$^1/_3\beta_T$
quadratic Stark effect in the cavity field	$\sim^1/_2\Delta\alpha E^2$	$-[2.7 \times 10^3\Delta\alpha/M_w][\phi(\epsilon) - \phi(n^2)]$	$\sim(\nu_{max} - \nu_0)$	$^2/_3\beta_T$
linear Stark effect in the reaction field	$\sim(\mu_g - \mu_e \cos\gamma)E$	$[1.26 \times 10^4\mu_g(\mu_g - \mu_e \cos\gamma)/M_w][\phi(\epsilon) - \phi(n^2)]$	$\sim(\nu_{max} - \nu_0)$	$^1/_3\beta_T$
repulsive forces	$\sim\exp(1/r)$; $\sim r^{-12}$	?	50−100 cm^{-1}	$4\beta_T$

[a] ν_{max}, band maximum; ν_0, 0−0 energy of the free solute; α_s, polarizability of the solvent molecule; $\Delta\alpha$, polarizability difference between the ground and the excited states of the solute; r, distance between the molecules; M_w, molecular weight stands for the cubed Onsager radius, according to ref 24; $\phi(n^2)$, Lorentz−Lorenz function of the refractive index; μ_g, μ_e, γ, dipole moments of the solute in the ground and the excited states, respectively, and the angle between them; E, electric field strength; φ, the angle between the direction of E and the vector of the dipole moment difference; $\phi(\epsilon) = (\epsilon - 1)/(\epsilon + 2)$, ϵ, dielectric constant of the matrix in the liquid state. [b] Reference 20. [c] Slope of the pressure shift coefficient dP/dν vs the hole burning frequency ν; β_T, isothermal volume compressibility. [d] Empirically, the cavity field in dipolar liquids is proportional to $[\phi(\epsilon) - \phi(n^2)]^{1/2}$.[20,28]

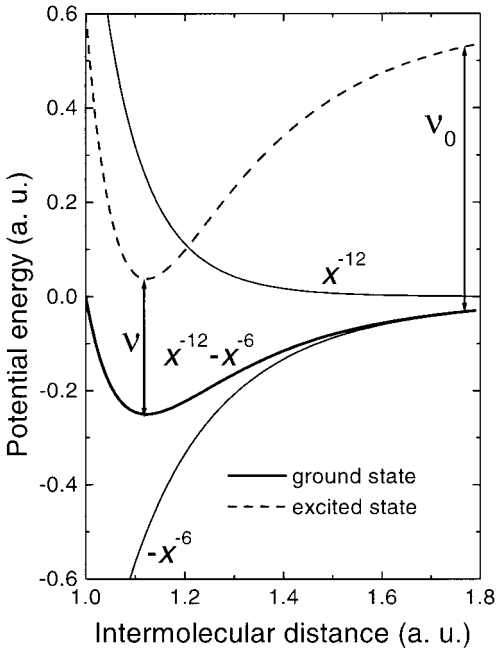

Figure 2. Potential energy diagram for the interaction between a spherical solute and a spherical solvent molecule. The separation of attractive and repulsive contributions is possible as far as the model functions have been defined for both. Here power laws are applied to the ground state (the Lennard-Jones potential). In the systems with dispersive solvent shifts ($\nu < \nu_0$) the potential well is deeper and the attractive branch is steeper in the excited state, but little is known about the behavior of the repulsive interaction (see text for discussion).

n-alkanes.[17−19,24,25] Both ν_0 and $\Delta\alpha$ can be estimated from the intercept and slope (p, further on referred to as the Bakshiev number, Table 2) of such a plot, respectively.[17,24] The effects of polarity are exposed best in a solvent set with approximately constant n, while the dielectric permittivity ϵ is changed.[17,24]

In polycyclic aromatic hydrocarbons the dispersive red shift largely prevails, the Bakshiev number being in the range of −1000 to −2000, −4000 to −5000, and −6000 to −9000 cm^{-1} for ^1L_b (α), ^1L_a (p), and ^1B_b(β) types of transitions, respectively.[24] In highly polar liquids an additional small (about 10% of the dispersive shift) bathochromic displacement appears due to the quadratic Stark effect in the cavity field.[27,28]

In free-base porphyrins the dispersive shift of the first absorption band is small: $p = -128$, −336, −639, and −659 cm^{-1} for octaethylporphine (OEP), porphine, tetraphenylporphine (TPP), and chlorin, respectively (Table 2).[18,19,34] The substitution of the methine group (CH) at the meso position to nitrogen atoms greatly enhances both the oscillator strength and polarizability of the S_1 state ($p = -988$ cm^{-1} for *t*-Bu-TAP, Figure 3), especially when accompanied with annelation of benzo groups to the pyrrolic rings yielding phthalocyanine ($p = -2240$ cm^{-1}).[34]

For free-base tetrapyrrolic pigments a peculiar hypsochromic shift of the S_1 (Q_y) band appears in polar media, while the second transition (Q_x) undergoes a bathochromic displacement.[18,19] These effects have been ascribed to the shift of hydrogen atoms closer to each other in a polar environment as a result of a decrease of their mutual electrostatic repulsion.[18,19] Figure 3 shows that in *t*-Bu-TAP all polar solvents cause a strong deviation to the higher energies with respect to the solvatochromic plot of *n*-alkanes. As in the case of OEP and TPP,[18,19] the molecules with quadrupolar moments (dioxane, toluene) produce a similar effect. Interestingly, the protic media deviate less from the *n*-alkane line than the aprotic solvents with the same polarity and polarizability (cf. acetonitrile and methanol, aceton and ethanol).

(2) Mechanisms of Inhomogeneous Broadening. The inhomogeneous bandwidth and the band shift have the same origin: the matrix-induced changes in optical transition energies. The correlations between the shifts of band maxima and the widths are of interest,[20,25] since the linear Stark effect in the cavity field, the repulsive solute−solvent interactions, and the conformational flexibility of dye molecules appear strongly in broadening, but weakly or not at all in band shifts.

In nonpolar solvent glasses the width of inhomogeneous site distribution function (IDF) is about 10% of the total solvent shift (plus a residual value of ~100 cm^{-1}).[20] It is worth noting that glasses contain about 10% of free space corresponding on the average to a single vacancy among ~10 solvent molecules in the closest coordination layer of the solute. On the other hand, in dipolar hosts the matrix fields lead to the shift and broadening of IDF of comparable magnitude (Table 1).[20]

Figure 4 shows the relationship between the double value of the half-width at half-maximum for the long-wavelength slope of the band (2HWHM) and the absolute solvent shift of the band maximum for different chromophores in the PMMA matrix (see also Table 2). The approximate linear dependencies for the widths of IDF in 1,3-dimethylcyclohexane and propylene carbonate glasses[20] are depicted for comparison. In PMMA the bands are even broader than in a very polar solvent glass, propylene carbonate. Separately, it was established that the width of IDF and the bandwidth are similar (within 10%), if the linear electron−phonon coupling is weak (the Debye−Waller factor is larger than 0.5), so the value of 2HWHM is used instead of IDF. For relatively rigid structures (OEP, chlorin, 3,4-benzopyrene (3,4-BP), 9,10-dichloroanthracene (9,10-ClA)) a roughly

TABLE 2: Spectroscopic Characteristics of Dopant Molecules in PMMA Host Matrix at 6 K

dopant	ν_0[a] (cm^{-1})	ref[b]	$\nu_{max} - \nu_0$[c] (cm^{-1})	2HWHM[d] (cm^{-1})	$(d\nu/dP)_{max}$[e] (GHz/bar)	$-p$[f] (cm^{-1})
octaethylporphine	16 056 ± 5 (s)	19	182	160	0.055	128 ± 19
tetraphenylporphine	15 617 (j)	33	−38	276	−0.118	639 ± 40
	15 613 ± 9 (s)	18,19				
t-Bu-TAP	16 326 ± 9 (s)	34	−87	328	−0.260	988 ± 39
chlorin	15 912 (j)	35	−97	230	−0.121	659 ± 20
	15 857 ± 5 (s)	19				
t-Bu-Pc	14 828 ± 34 (s)	19	−387	374	−0.503	1918 ± 138
t-Bu-Pc/PEld[h]			−492	192	−0.45	
3,4-benzopyrene	25 265 (j)	36	−453	246	−0.235	1567 ± 60
	25 202 ± 15 (s)	17				
Pc/PEld[h]	15 132 (j)	37	−687	92	−0.451	2240 ± 59[i]
	15 022 ± 14 (s)[i]	34				
squarene dye	16 358 ± 20 (s)	*g*	−721	354	−0.325	2617 ± 84
9,10-dichloroanthracene	25 950 (j)	38	−1328	362	−0.855	4175[j]

[a] Transition frequency of free dopant measured in supersonic jet (j) or estimated from the solvent shifts at room temperature (s). [b] Source of ν_0. [c] Band maximum in PMMA relative to the vacuum frequency. [d] Double value of the half-width at half-maximum of the red side of the band, error ±10 cm^{-1}. [e] Pressure shift coefficient of the hole burned at the band maximum. [f] Bakhshiev number (slope of eq 1 in liquid *n*-alkanes), this work and from refs 17, 19, 24, and 34. [g] This work. [h] In low-density polyethylene. [i] Measured in fluorescence. [j] For anthracene, ref 24.

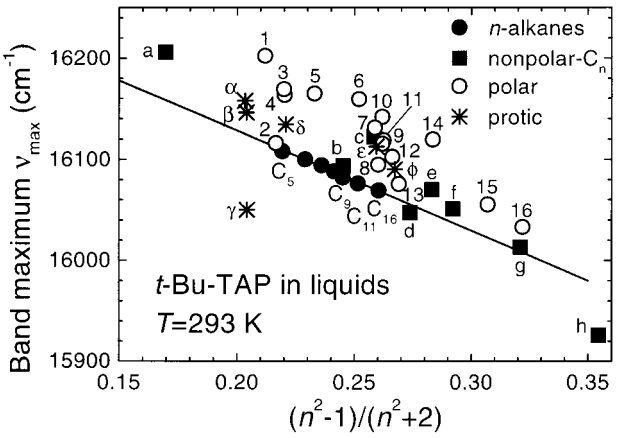

Figure 3. Dependence of the *t*-Bu-TAP absorption maxima at room temperature on the Lorentz−Lorenz function of the solvent (*n*-alkanes (●) from pentane (C_5) to hexadecane (C_{16})), nonpolar solvents other than *n*-alkanes (■) (a, C_8F_{18}; b, 2,3,4-trimethylpentane; c, dioxane; d, CCl_4; e, 1,3-dimethyladamantane; f, toluene; g, hexachlorobutadiene; h, CS_2), polar solvents (○) (1, CH_3CN; 2, $(C_2H_5)_2O$; 3, $(CH_3)_2CO$; 4, CH_3COOCH_3; 5, CH_3NO_2; 6, propylene carbonate; 7, dimethylformamide; 8, $CH_3CH_2CH_2Br$; 9, cyclopentanone; 10, γ-butyrolactone; 11, epichlorhydrin; 12, CH_2ClCH_2Cl; 13, $CCl_3COOC_2H_5$; 14, $(CH_3)_2SO$; 15, furfural; 16, $C_6H_5NO_2$), protic solvents (∗) (α, CH_3OH; β, H_2O/CH_3OH (25% (v/v)); γ, H_2O/CH_3OH (33% (v/v)); δ, C_2H_5OH; ϵ, *N*-methylformamide; φ, formamide). The line is a linear regression for *n*-alkanes with intercept 16 326 ± 9 cm^{-1} and slope −988 ± 39 cm^{-1}.

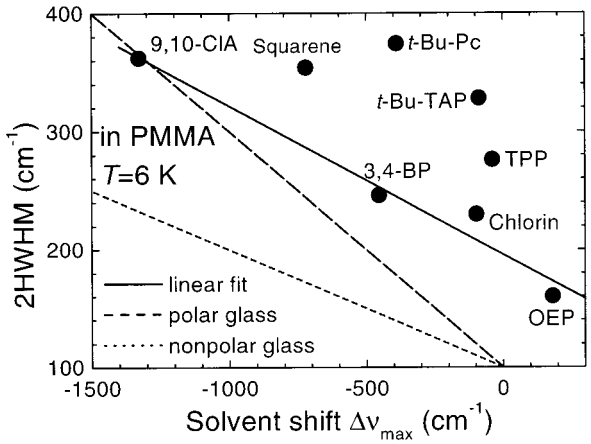

Figure 4. Dependence of inhomogeneous bandwidth on the vacuum-to-matrix shift of the absorption maximum in PMMA host matrix at 6 K. For relatively rigid structures (OEP, chlorin, 3,4-BP, 9,10-ClA) a linear correlation is obtained (eq 13). The lines represent the inhomogeneous broadening due to the dispersive interaction in glassy nonpolar 1,3-dimethylcyclohexane and both the dispersive and quadratic Stark effects in highly polar propylene carbonate, respectively.[20]

linear dependence between 2HWHM and $\Delta\nu_{max}$ holds:

$$[\text{2HWHM}] = (196 \pm 12) - (0.126 \pm 0.016)\Delta\nu_{max}; \quad N = 4,\ r = 0.983 \quad (13)$$

where *N* is the number of data points and *r* is the correlation coefficient.

A distinctive feature of eq 13 is the intercept as large as 196 cm^{-1} in PMMA. Such residual broadening of about 100 cm^{-1} occurs even in nonpolar aliphatic hydrocarbon glasses for α (^1L_b) type transitions of arenes (pyrene)[20] and porphyrins (octaethylporphine, chlorin) that are accompanied with very small polarizability changes and dispersive solvent shifts. We assume that either repulsive forces or bond dipole interactions should be responsible for this large additional inhomogeneity.

There is little doubt that an additional reason for broadening can be the distortion of the molecular backbone, e.g. in the squarene dye, or flexible phenyl substituents in the meso position of tetraphenylporphine. The bulky *tert*-butyl substitution in the periphery of TAP and phthalocyanine (Pc) seems to cause significant disorder, since even in nonpolar polyethylene host matrix, the 2HWHM of *t*-Bu-TAP (155 cm^{-1}) and *t*-Bu-Pc (192 cm^{-1}) is much larger than that of chlorin (84 cm^{-1}) or Pc (92 cm^{-1}) (Table 2). By contrast, in (quadru)polar polystyrene the influence of substituents is much less pronounced, with the 2HWHM at 6 K for a pair of solutes TAP/*t*-Bu-TAP equal to 254/266 cm^{-1} and for Pc/*t*-Bu-Pc to 264/294 cm^{-1}. The broadening in PS is probably induced by strong polar solvation effects in the central part of the macrocycle (see the previous section).

The mechanisms of inhomogeneous broadening can be rather complex and should be taken into account properly when treating the pressure shifts of holes burned within the bands.

(3) Pressure Shifts on Holes in PMMA Doped with Different Dyes. The measurements were carried out in films cast of commercial Plexiglass, an amorphous high-molecular

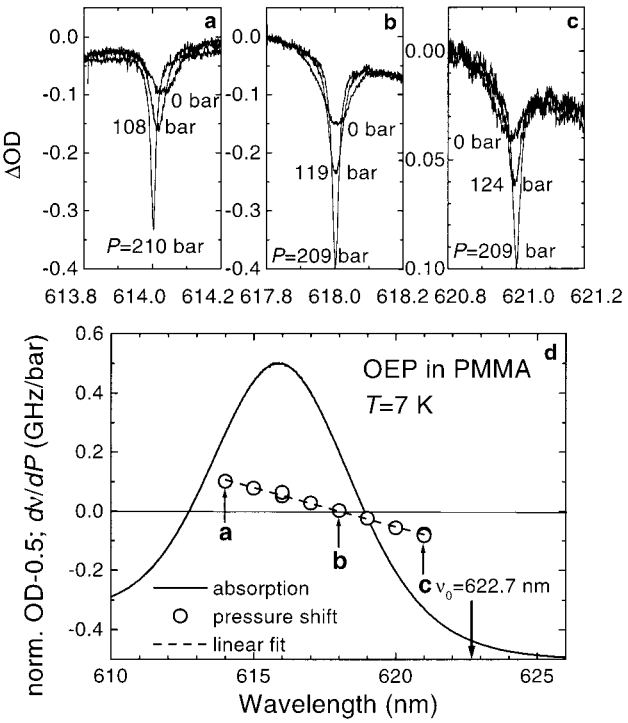

Figure 5. Low-temperature absorption spectrum and the pressure shift coefficients as a function of the burning wavelength of spectral holes for octaethylporphine doped in PMMA (d). The broadening and shift of holes after the pressure is released is illustrated in panels a−c. Note that the pressure shift changes sign at 618 nm, where only broadening takes place (b). The 0−0 origin in nonsolvated OEP is indicated by an arrow.

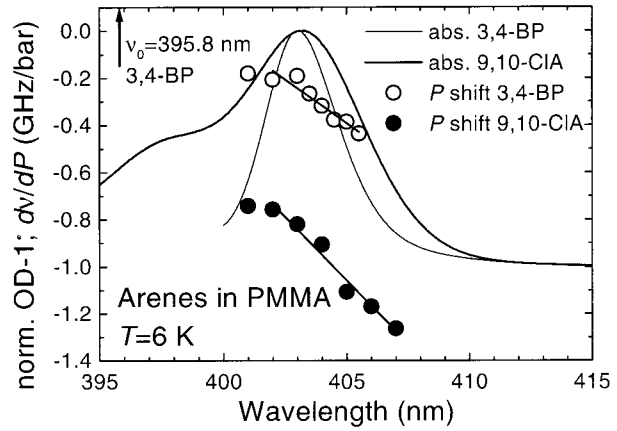

Figure 6. Low-temperature absorption spectra and the pressure shift coefficients as a function of the burning wavelength of spectral holes for 3,4-benzopyrene and 9,10-dichloroanthracene doped in PMMA. The 0−0 origin of 3,4-BP in a cold molecular beam at 395.8 nm is indicated by an arrow;[36] the ν_0 of 9,10-ClA lies far outside the wavelength range (385.4 nm [38]).

weight PMMA. Most of the compounds lacking the intrinsic photochemistry are subject to hole burning in highly polar PMMA, although with low yield and dispersive photoconversion kinetics. The holes burned under He gas pressure of 200 bar shift and broaden if the pressure is released (Figure 5). The hole shift is a perfectly linear function of ΔP. A well-known dependence of the pressure shift coefficient ($d\nu/dP$) on wavelength (the so-called color effect[13−16]) is observed (Figures 5−8).

The pressure shift coefficient $d\nu/dP$ measured at the absorption maximum depends linearly on the absolute vacuum-to-matrix frequency shift $\Delta\nu_{max}$ (Figure 9):

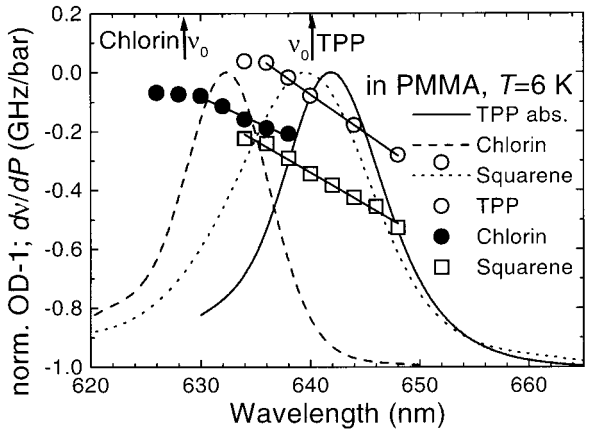

Figure 7. Low-temperature absorption spectra and the pressure shift coefficients as a function of burning wavelength of spectral holes for the squarene dye, chlorin, and tetraphenylporphine doped in PMMA. The 0−0 origins of chlorin and TPP in a cold molecular beam are indicated by arrows;[33,35] the ν_0 of the squarene dye lies outside the wavelength range (611.3 nm).

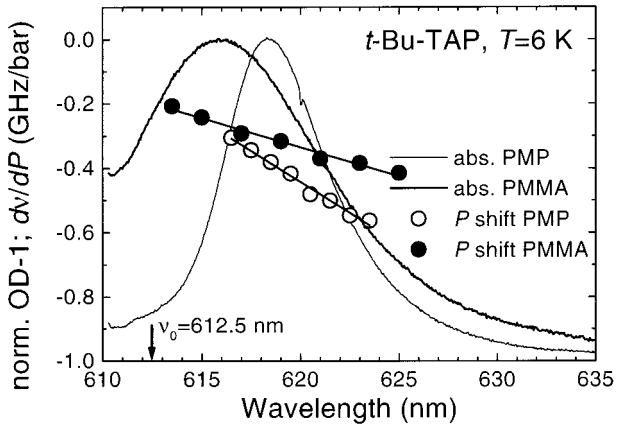

Figure 8. Low-temperature absorption spectra and the pressure shift coefficients as a function of burning wavelength of spectral holes of *t*-Bu-TAP doped in PMMA and poly(4-methyl-1-pentene). The 0−0 origin in nonsolvated *t*-Bu-TAP is indicated by an arrow.

$$(d\nu/dP)_{max} = (-0.101 \pm 0.053) + (5.26 \pm 0.89) \times 10^{-4}\Delta\nu_{max}; \quad N = 9, r = 0.913 \quad (14)$$

The slope (5.26 ± 0.89) × 10^{-4} GHz bar^{-1} cm or 1.8 × 10^{-5} bar^{-1} is quite close to double compressibility $2\beta_T$ of PMMA equal to 2.6 × 10^{-5} bar^{-1},[11] in accordance with the dispersive solvent shift mechanism (eq 6).

For most of the dopants both the pressure and solvent shifts are bathochromic, except for OEP. Another simple porphyrin, tetraphenylporphine, shows a blue shift of holes burned on the short-wavelength edge of the band (Figure 7). At a certain position the hole shows only broadening but no shift (Figure 5). For the remaining compounds the position where no *P* shift is expected ($\nu_{0(P)}$) can be established by extrapolation. In Table 3 the no-shift frequencies are compared with the 0−0 transition energies of nonsolvated dyes, obtained from free jet experiments[33,35−38] or solvatochromic measurements at room temperature.[17,19,34] Concerning the difference $\nu_{0(P)} - \nu_0$, the data fall into two groups: in tetrapyrroles the $\nu_{0(P)}$ is blue-shifted with respect to ν_0, whereas a large negative deviation occurs for the other chromophores (3,4-BP, 9,10-ClA, and squarene dye). In the dopants other than tetrapyrroles $\nu_{0(P)}$ is located approximately a halfway between ν_0 and the band maximum.

The slopes of the linear plots of pressure shift coefficients

TABLE 3: Frequency Dependence of Pressure Shift Coefficients of Spectral Holes in the PMMA Host Matrix at 6 K

dopant	$\nu_{0(P)}$[a] (cm^{-1})	$\nu_{0(P)} - \nu_0$[b] (cm^{-1})	$d(d\nu/dP)/d\nu$[c] (10^{-5} bar^{-1})	N[d]	r[e]	data interval (nm)
chlorin	15 992 ± 17	80 ± 17	2.25 ± 0.17	5	0.992	630−638
t-Bu-TAP	16 588 ± 29	262 ± 29	2.42 ± 0.17	5	0.991	613.5−623
squarene dye	16 004 ± 17	−357 ± 17	2.96 ± 0.12	8	0.995	634−648
t-Bu-Pc	14 926 ± 78	98 ± 78	3.1 ± 0.5	6	0.953	687−700
octaethylporphine	16 181 ± 2	125 ± 2	3.37 ± 0.08	10	0.9975	614−621
tetraphenylporphine	15 694 ± 2	77 ± 2	3.59 ± 0.05	5	0.9997	636−648
3,4-benzopyrene	24 989 ± 35	−276 ± 35	4.05 ± 0.6	7	0.952	402−405.5
9,10-dichloroanthracene	25 275 ± 46	−675 ± 46	5.9 ± 0.5	6	0.987	402−407

[a] Frequency at which spectral hole shows no pressure shift. [b] ν_0, transition frequency of free dopant (see Table 2). [c] Slope of the linear dependence of the pressure shift coefficients $d\nu/dP$ vs hole burning frequency ν. [d] Number of data points. [e] Linear regression coefficient.

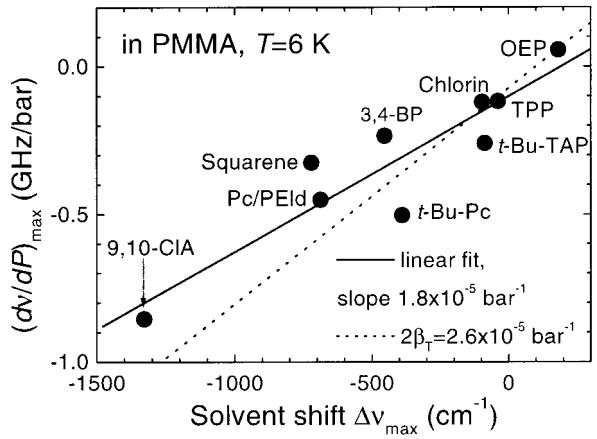

Figure 9. Pressure shift coefficients of spectral holes burned at the absorption band maxima as a function of solvent shift for solutes doped in PMMA (Pc/PEld—phthalocyanine in polyethylene) (Table 2). The dotted line has a slope of the double compressibility ($2\beta_T$) of PMMA at 4 K.[11]

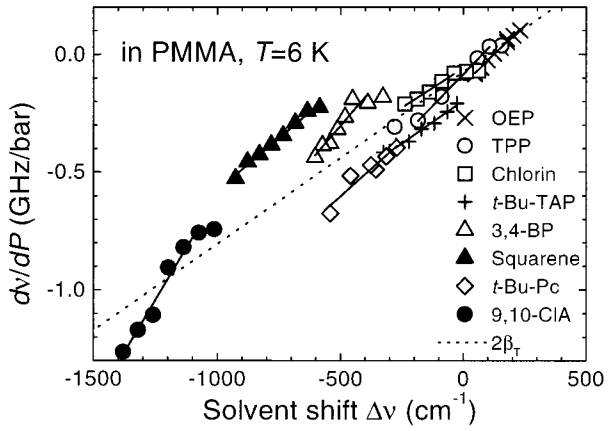

Figure 10. Pressure shift coefficients of spectral holes burned over the inhomogeneous bands of chromophores in PMMA host matrix plotted as a function of absolute solvent shifts. The linear regression lines have steeper slopes (Table 3) than the double compressibility of PMMA at 4 K (dotted line).

vs the hole burning frequency are given in Table 3 and illustrated in Figure 10. In several systems the deviating points corresponding to the edges of the band have been excluded from the linear regression of $d\nu/dP$ vs ν. For *t*-Bu-TAP the slope of the dependence under discussion ($d(d\nu/dP)/d\nu = 2.42 \times 10^{-5}$ bar^{-1}) is very close to the double value of isothermal compressibility of bulk PMMA at 4 K ($2\beta_T = 2.6 \times 10^{-5}$ bar^{-1})[11] (Table 4), in accordance with the dispersive solvent shift mechanism (eq 7). However, the change of pressure coefficient for the remaining chromophores (except for chlorin) over the inhomogeneous band is remarkably larger. The steepness of this dependence is also the reason for $\nu_{0(P)}$ being smaller than ν_0 in solutes other than free-base tetrapyrroles. Such a high sensitivity of $d\nu/dP$ with respect to the hole position within the inhomogeneous band is unexpected, bearing in mind that the matrix shift mechanisms other than attractive London forces lead to the slopes much less than $2\beta_T$ (Table 1).

We are inclined to think that the repulsive interactions can be responsible for the slopes steeper than $2\beta_T$. Obviously both the attractive and repulsive interactions are subject to statistical spread in the disordered environment. Particularly strong frequency dependence is expected if both types of forces are correlated (eq 10). Some degree of correlation is definitely realized, since the guest molecules surrounded by a tight solvent cage are subject to both strong London and exchange forces.

(4) Pressure Shifts on Holes in Polymers Doped with *t*-Bu-TAP. The availability of isothermal compressibilities (bulk moduli) for a number of polymers at 4.2 K[11] enables one to test the expressions describing the inhomogeneous pressure effects (eqs 7, 10, and 12, Table 1). The pressure shift coefficients display a linear relationship with hole burning frequency (Figure 8). The respective slopes are very close to $2\beta_T$ for isotropic polymers (Table 4, Figure 11):

$$d(d\nu/dP)/d\nu = (-1.32 \pm 0.22) \times 10^{-5} + (1.37 \pm 0.07)[2\beta_T]; \quad N = 5, r = 0.9964 \quad (15)$$

By contrast, optically turbid plastics, such as polyethylene, Nylon 6, and poly(oxymethylene) have the experimental slope values larger than $2\beta_T$. These light scattering polymers consist of amorphous and crystalline domains with different optical and mechanical properties. The optical probe molecules reside in the glassy regions of the matrix that have evidently higher compressibility than the average value for a mixture of amorphous and crystalline domains.

Despite the nice agreement between the slopes and the bulk compressibilities, the zero-shift frequencies deviate considerably from the purely electronic origin of *t*-Bu-TAP in a vacuum (16 326 cm^{-1}). The differences $\nu_{0(P)} - \nu_0$ are the smallest for nonpolar polyolefins (65 cm^{-1} in PEld and 99 cm^{-1} in PMP) and increase with growing polarity of the polymer, e.g. 204 cm^{-1} for PVB and 287 cm^{-1} for PMMA. A large hypsochromic shift of band maxima is obvious also in polar liquid solvents (Figure 3) (see above). Moreover, the polarity of the matrix leads to a pronounced broadening of spectral bands from 155 cm^{-1} in PEld to 328 cm^{-1} in PMMA. Since the field effects yield the slope values that are considerably smaller than $2\beta_T$ (eq 12, Table 1), it is evident that in the present case the "correct" value is obtained as a consequence of compensation phenomena. In other words, the interaction producing a dependence of $d\nu/dP$ on ν steeper than $2\beta_T$ should be present also in polymer hosts other than PMMA.

TABLE 4: Frequency Dependence of the Pressure Shift Coefficients of Spectral Holes in *t*-Bu-TAP in Polymer Host Matrices at 6 K

	band properties		characteristics of pressure shift						
host[a]	$\nu_{max} - \nu_0$[b] (cm^{-1})	2HWHM[c] (cm^{-1})	$(d\nu/dP)_{max}$[d] (GHz/bar)	$\nu_{0(P)} - \nu_0$[e] (cm^{-1})	$d(d\nu/dP)/d\nu$[f] (10^{-5} bar^{-1})	$2\beta_T$[g] (10^{-5} bar^{-1})	N[h]	r[i]	data interval (nm)
Nylon 11	−173	258	−0.238	226 ± 42	1.9 ± 0.19	2.41	7	0.977	615.5−624.5
Nylon 6	−178	276	−0.245	190 ± 23	2.19 ± 0.13	2.06	6	0.993	614.5−624.5
PVB	−136	262	−0.244	204 ± 25	2.35 ± 0.15		7	0.989	614.5−623.5
PVC	−142	259	−0.277	244 ± 20	2.38 ± 0.11	2.74	5	0.997	616−622
PMMA	−87	328	−0.263	287 ± 27	2.42 ± 0.17	2.60	6	0.991	613.5−623
polyoxymethylene	−118	290	−0.207	150 ± 8	2.56 ± 0.07	1.59	8	0.998	613.5−624.3
Teflon AF	−28	240	−0.195	149 ± 21	3.51 ± 0.30		8	0.978	612.5−619.5
polystyrene	−182	261	−0.39	183 ± 22	3.54 ± 0.2	3.57	6	0.994	615.5−625.5
PEld	−190	155	−0.279	65 ± 10	3.62 ± 0.15	2.82	9	0.994	615−623
PEld/Chl[j]	−177	84	−0.173	−45 ± 4	4.38 ± 0.12		6	0.9986	633−638
PEld/Pc[j]	−687	92	−0.451	−345 ± 22	4.36 ± 0.27		4	0.996	691−694
PEld/*t*-Bu-Pc[j]	−492	192	−0.450	383 ± 169	1.41 ± 0.29		7	0.91	692−698
PMP	−154	196	−0.380	99 ± 13	4.94 ± 0.2	4.55	8	0.995	616.5−623.5

[a] PVB, poly(vinylbutyral-*co*-vinyl alcohol-*co*-vinyl acetate); PVC, poly(vinyl chloride); PMMA, poly(methyl methacrylate); PEld, low-density polyethylene; PMP, poly(4-methyl-1-pentene). [b] Absorption maximum relative to the 0−0 origin in free *t*-Bu-TAP ($\nu_0 = 16\,326$ cm^{-1}), error ±5 cm^{-1}. [c] Double value of the half-width at half-maximum of the red side of the band, 2HWHM, error ±10 cm^{-1}. [d] Pressure shift coefficient of the hole burned at the band maximum. [e] Frequency at which no pressure shift occurs (relative to the 0−0 origin in free *t*-BuTAP). [f] Slope of the linear dependence of the pressure shift coefficient vs the hole burning frequency. [g] Double value of isothermal compressibility of bulk polymers from ref 11. [h] Number of data points (holes). [i] Linear regression coefficient. [j] Dopants other than *t*-Bu-TAP.

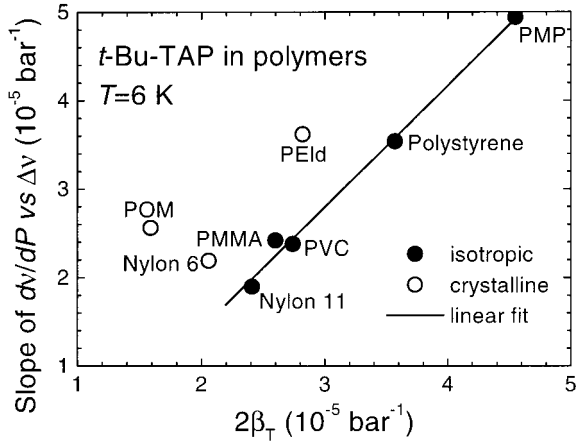

Figure 11. Slopes of the linear plots of pressure shift coefficients vs the hole burning frequency for *t*-Bu-TAP compared to the double compressibility of polymers at 4 K (Table 4).

Therefore, the dependence of the pressure shift coefficient on the absolute solvent shift is governed by a superposition of several intermolecular interaction mechanisms: the attractive dispersion forces that yield the slope of $2\beta_T$, the repulsive branch that is responsible for a steep ($4\beta_T$) slope, and the Stark effects in the cavity field giving rise to strong inhomogeneous broadening and shallow slopes less than β_T.

Conclusions

The pressure-induced shifts of spectral holes burned in the 0−0 bands of a number of chromophores doped in polymer host matrices were investigated. Fairly large sets of polymers with known low-temperature compressibilities[11] and dyes with widely different vacuum-to-solid shifts were chosen for measurements. Solvatochromic mechanisms have different solute−solvent distance dependencies. Therefore, the P shifts of spectral holes plotted as a function of burning frequency can serve as a sensitive measure of intermolecular potentials. In principle, at least two mechanisms ought to be involved, an attractive and a repulsive one. In reality, the solvent shifts are more complex. The expressions for $dP/d\nu$ were derived for dispersive, electric field-induced, and repulsive effects. A strong dependence of $dP/d\nu$ on hole burning wavenumber is expected for the dispersive interaction, since both the matrix polarizability and the Onsager radius change when pressure is applied. In accordance with the results obtained earlier,[12−14] the slope of the linear relationship between $d\nu/dP$ and $\Delta\nu$ must be equal to $2\beta_T$. The cavity and reaction fields yield a smaller P dependence, since the local electric field strength scales as one-third of the matrix compressibility β_T.

In contrast to the predictions, the sensitivity of P shift coefficients with respect to the burning wavelength is frequently higher than $2\beta_T$. The most probable cause of such a deviation stems from the repulsive forces between the molecules. An alternative, but definitely less universal, reason may be the reaction fields created by quadrupolar moments or the bond dipoles.

The determination of 0−0 origins of nonsolvated molecules as well as the matrix compressibilities on the basis of hole burning experiments is conceivable provided the guest−host interactions are well-understood in both the ground and the excited states. The β_T is best estimated by using spectral holes at the band maxima of several impurities with different solvent shifts rather than from a set of holes created over an inhomogeneous band of a single probe molecule. Unfortunately, the free-base porphyrins that are favorable because of their intrinsic photochemistry possess a complex solvatochromic behavior.

The simultaneous consideration of pressure and electric field effects[39] on spectral holes will undoubtedly help to specify the types of intermolecular interactions involved. Room temperature solvent shift studies in liquids of variable polarity and polarizability can yield also very helpful insight into the forces influencing the solute spectra in condensed phase.[24]

Acknowledgment. I would like to thank Professor Urs P. Wild for continuous support and encouragement during my stay in the Physical Chemistry Laboratory, ETHZ. I am very grateful to Bruno Lambillotte and Roland Schmidli (ETHZ) for help in designing the pressure cell and its skillful machining. This work was supported in part by the "Board of the Swiss Federal Institutes of Technology", ETH Zürich, and the Estonian Science Foundation Grant No. 3869.

References and Notes

(1) The experimental part of this work was carried out in the Physical Chemistry Laboratory, Swiss Federal Institute of Technology (ETHZ), CH-8092 Zürich, Switzerland.

(2) Brey, L. A.; Schuster, G. B.; Drickamer, H. G. *J. Chem. Phys*. **1979**, *71*, 2765.

(3) Samara, G. A.; Riggleman, B. M.; Drickamer, H. G. *J. Chem. Phys*. **1962**, *37*, 1482.

(4) Offen, H. W. In *Organic Molecular Photophysics*, Vol. 1; Birks, J. B., Ed.; Wiley-Interscience: New York, 1973; pp 103−151.

(5) Okamoto, B. Y.; Drickamer, H. G. *J. Chem. Phys*. **1974**, *61*, 2870.

(6) Politis, T. G.; Drickamer, H. G. *J. Chem. Phys*. **1981**, *74*, 263.

(7) Park, E. H.; Kadhim, A. H.; Offen, H. W. *Photochem. Photobiol*. **1968**, *8*, 261.

(8) Ellervee, A.; Jaaniso, R.; Kikas, J.; Laisaar, A.; Suisalu, A.; Shcherbakov, V. *Chem. Phys. Lett*. **1991**, *176*, 472.

(9) Sesselmann, Th.; Richter, W.; Haarer. D. *J. Lumin*. **1987**, *36*, 263.

(10) Sesselmann, Th.; Richter, W.; Haarer. D.; Morawitz, H. *Phys. Rev. B* **1987**, *36*, 7601.

(11) Perepechko, I. I. *Low-Temperature Properties of Polymers*; Mir Publishers: Moscow, 1980.

(12) Laird, B. B.; Skinner, J. L. *J. Chem. Phys*. **1989**, *90*, 3274.

(13) Gradl, G.; Zollfrank, J.; Breinl, W.; Friedrich, J. *J. Chem. Phys*. **1991**, *94*, 7619.

(14) Pschierer, H.; Friedrich, J.; Falk, H.; Schmitzberger, W. *J. Phys. Chem*. **1993**, *97*, 6902.

(15) Zollfrank, J.; Friedrich, J.; Fidy, J.; Vanderkooi, J. M. *J. Chem. Phys*. **1991**, *94*, 8600.

(16) Friedrich, J.; Gafert, J.; Zollfrank, J.; Vanderkooi, J.; Fidy, J. *Proc. Natl. Acad. Sci*. **1994**, *91*, 1029.

(17) Renge, I. *J. Photochem. Photobiol*. *A* **1992**, *69*, 135.

(18) Renge, I. *Chem. Phys. Lett*. **1991**, *185*, 231.

(19) Renge, I. *J. Phys. Chem*. **1993**, *97*, 6582.

(20) Renge, I.; Wild, U. P. *J. Lumin*. **1996**, *66* and *67*, 305.

(21) Koppel, I. A.; Palm, V. A. In *Advances in Linear Free Energy Relationships*; Chapman, N. B., Shorter, J., Eds.; Plenum: London, 1972; Chapter 5, pp 203−280.

(22) Renge, I. *J. Chem. Phys*. **1997**, *106*, 5835.

(23) Bakshiev, N. G.; Girin, O. P.; Piterskaya, I. V. *Opt. Spektrosk*. **1968**, *24*, 901 [*Opt. Spectrosc*. **1968**, *24*, 483].

(24) Renge, I. *Chem. Phys*. **1992**, *167*, 173.

(25) Renge, I. *J. Phys. Chem*. **1995**, *99*, 15955.

(26) Böttcher, C. J. F. *Theory of Electric Polarization*, Vol. I; Elsevier: Amsterdam, 1973.

(27) Nicol, M.; Swain, J.; Shum, Y.-Y.; Merin, R.; Chen, R. H. H. *J. Phys. Chem*. **1968**, *48*, 3587.

(28) Renge, I.; van Grondelle, R.; Dekker: J. P. *J. Photochem. Photobiol*. *A* **1996**, *96*, 109.

(29) Renge, I. *J. Opt. Soc. Am. B* **1992**, *9*, 719.

(30) McCarty, M., Jr.; Robinson, G. W. *Mol. Phys*. **1959**, *2*, 415.

(31) Sverdlova, O. V.; Bakhshiev, N. G. *Opt. Spektrosk*. **1977**, *42*, 288.

(32) Zipp, A.; Kauzmann, W. *J. Chem. Phys*. **1973**, *59*, 4215.

(33) Even, U.; Magen, J.; Jortner, J.; Friedman, J.; Levanon, H. *J. Chem. Phys*. **1982**, *77*, 4374.

(34) Renge, I.; Wolleb, H.; Spahni, H.; Wild, U. P. *J. Phys. Chem*. *A* **1997**, *101*, 6202.

(35) Even, U.; Jortner, J. *J. Chem. Phys*. **1982**, *77*, 4391.

(36) Greenblatt, G. D.; Nissani, E.; Zaroura, E.; Haas, Y. *J. Phys. Chem*. **1987**, *91*, 570.

(37) Fitch, P. S. H.; Wharton, L.; Levy, D. H. *J. Chem. Phys*. **1979**, *70*, 2018.

(38) Hirayama, S.; Iuchi, Y.; Tanaka, F.; Shobatake, K. *Chem. Phys*. **1990**, *144*, 401.

(39) Altmann, R. B.; Renge, I.; Kador, L.; Haarer, D. *J. Chem. Phys*. **1992**, *97*, 5316.